Analytical model for wave-related transport

Judith Bosboom[1,2], Gert Klopman[3,2], Ad Reniers[1,2], Marcel J.F. Stive[1,2]

Abstract

A computationally efficient, analytical model to determine net sediment transport rates in oscillatory flow is presented. The model is based on (approximate) analytical solutions to the 1DV momentum and advection-diffusion equations and on the subsequent analytical integration of the sediment flux over time and depth. The model is validated against measurements of sediment concentrations and net transport rates performed in WL|DELFT HYDRAULICS' Large Oscillating Water Tunnel (LOWT). Further, comparisons are made with the predictions of numerical 1DV models and sediment transport formulae. The model gives accurate estimates of the net transport rates for medium sand. For finer sand, although qualitatively correct, the model fails to predict the strong offshore sediment transport rates at higher velocities, mainly due to limitations of the diffusion approach for the upward transport of sediment.

Introduction

A variety of concepts is used in morphodynamic models to describe the wave-related transport, i.e. the transport related to the correlation between sediment concentration and long wave motions as well as to wave asymmetry and time lag effects between wave orbital velocity and concentration within the wave cycle.

In quasi-steady models, instantaneous adaptation of the concentration to the time-varying near-bed velocity (or bed shear stress) is assumed such that the total load is directly related to some power of the instantaneous velocity. Assuming in addition that the velocity profile is reasonably uniform over the vertical, the vertically integrated flux can be schematised as the product of the velocity at some reference level and the total load, typically resulting in a formula in which the transport is proportional to some power of the instantaneous velocity, e.g. the Bagnold model (Bowen, 1980; Bailard, 1981). Although the neglect of phase-lag effects between velocity and concentration is potentially inaccurate, quasi-steady formulae are popular amongst morphodynamic modellers thanks to their simplicity and possibility to combine processes acting on different time-scales.

Experiments of Ribberink and Chen (1993) and Janssen et al. (1996) demonstrate that in asymmetric oscillatory sheet flow conditions, the net transport rates for fine sand decrease for increasing oscillatory velocities and ultimately even reverse. In contrast with the Bailard formula, the semi-unsteady formulation according to Dibajnia and Watanabe (1992)

[1] WL|DELFT HYDRAULICS (mailing adress), P.O. Box 177, 2600 MH Delft, The Netherlands. Judith.Bosboom@wldelft.nl
[2] Netherlands Centre for Coastal Research (NCK), Department of Civil Engineering and Geosciences, Delft University of Technology, Delft, The Netherlands
[3] Albatros Flow Research, P.O. Box 85, 8325 ZH Vollenhove, The Netherlands

qualitatively reproduces these unsteady effects (Janssen et al., 1996). The latter formulation combines an essentially quasi-steady approach with a schematised time lag effect. It was found that for coarse sand the results obtained with both formulae are almost identical.

A more general modelling approach requires the intra-wave-period modelling of the velocity and concentration fields using for instance 1DV models (e.g. Fredsøe et al., 1985; Davies et al., 1997). The direct use of such a detailed intra-wave transport model in a morphodynamic model is time-consuming from a computational point of view, especially when used to study the effects of irregularity of the waves and wave groups. This disadvantage is partly removed by making an initial effort of tabulating the results of the intra-wave model for a specific situation, after which the morphodynamic model is run at relatively low costs (Rakha et al., 1997). An alternative way to reduce the computational costs is to apply (semi-) analytical methods to account for the intra-wave effects on the net transport rates while still capturing the essential features of the unsteady transport, i.e. the strong vertical gradients in the near-bottom time-varying flow and concentration including the non-instantaneous response of the sediment.

The purpose of this work is to present an analytical model based on the equations underlying the 1DV unsteady models. By finding (approximate) analytical solutions for the oscillatory velocity $\tilde{u}(z,t)$ and the oscillatory concentration $\tilde{c}(z,t)$ in the near-bed wave boundary layer and analytically integrating over time and depth, the net transport rate $q_{wave} = \frac{1}{t_2-t_1}\int_{t_1}^{t_2}\int_z \tilde{u}\tilde{c}\,\mathrm{d}z\mathrm{d}t$ as a function of the depth is obtained. A similar approach has been taken by Nielsen (1988), who however assumes a depth-invariant oscillatory velocity, therewith neglecting one of the essential features, viz. the strong vertical variation of the oscillatory velocity close to the bed.

The oscillatory boundary layer structure is taken into account by using an (approximate) analytical solution to the wave boundary layer momentum equation using a time-invariant eddy viscosity approach. For the computation of the bed shear stress, the time-variation of the eddy viscosity is accounted for. The time- and depth-dependency of the concentration field is resolved by analytically solving the advection-diffusion equation using a time-invariant sediment diffusivity and a bottom boundary condition which is a function of the instantaneous bed shear stress. In this way we expect to account for the majority of the transport near the bed; the bed load transport is assumed to be small as compared to the suspended load contribution.

Although in principle the model can be applied for an arbitrary input series of the oscillatory near-bed velocity, the validation of the model as presented in this paper focuses on second order Stokes conditions in the absence of a mean current. Measurements in WL|DELFT HYDRAULICS' Large Oscillating Water Tunnel (LOWT) by Ribberink and Al-Salem (1994) and Ribberink and Chen (1993) are used for model validation. In addition, comparisons are made with 1DV numerical models and the transport formulae of Bailard (1981) and Dibajnia and Watanabe (1992).

Oscillatory boundary layer model

Equation of motion and boundary conditions

After Reynolds-averaging, the wave boundary layer approximation to the momentum equation, for a rough, fully turbulent wave boundary layer flow, reads:

$$\frac{\partial u - u_\infty}{\partial t} = \frac{\partial u_d}{\partial t} = -\frac{\partial \langle u'w' \rangle}{\partial z}, \tag{1}$$

in which $u = u(z,t)$ is the Reynolds-averaged horizontal velocity, $u_\infty = u_\infty(t)$ the free stream velocity outside the boundary layer and $u_d = u - u_\infty$ the deficit velocity. Note that only a

purely oscillatory motion is considered in this paper. Further, $-\langle u'w'\rangle = \tau_{zx}/\rho$ is the Reynolds shear stress representing the vertical flux of fluid momentum. Here ρ is the fluid density, u' and w' are the instantaneous velocity fluctuations in horizontal and vertical direction respectively, and the brackets denote averaging over the turbulence time-scale.

The turbulence fluxes are modelled according to the Boussinesq hypothesis as:

$$-\langle u'w'\rangle = \nu_{t,f}\frac{\partial u}{\partial z}, \tag{2}$$

where $\nu_{t,f}$ is the eddy viscosity or turbulence eddy diffusivity of fluid momentum which we assume is not influenced by the presence of suspended sediment.

The wave boundary layer equation (1) is solved subject to the no-slip boundary condition and the boundary condition of the wave velocity approaching the quasi-constant $(\partial/\partial z \approx 0)$ velocity prescribed by e.g. an irrotational theory at the edge of the wave boundary layer:

$$\begin{aligned} &u = 0 \qquad \text{at} \qquad z = z_0 = \frac{k_n}{30}; \\ &u \to u_\infty \text{ for} \qquad z \to \infty, \end{aligned} \tag{3}$$

where z_0 is the effective position of the bottom depending on the equivalent Nikuradse sand grain roughness k_n and where ∞ implies a distance far from the bed compared to the boundary layer thickness, but close to the bed compared to the water depth.

Eddy viscosity model

Using the Prandtl mixing-length hypothesis and assuming that in the immediate vicinity of the bed the mixing length l is proportional to the distance above the bottom, $l = \kappa z$, yields for the bed shear stress:

$$\tau_b(t) = \lim_{z\to 0}\left(\rho(kz)^2\left|\frac{\partial u}{\partial z}\right|\frac{\partial u}{\partial z}\right) \tag{4}$$

Using the Boussinesq hypothesis and realising that $\tau_b(t) = \rho|u_*(t)|u_*(t)$ gives for the eddy viscosity close to the bed $\nu_{t,n} = \kappa|u_*|z$. Trowbridge and Madsen (1984) demonstrated that the solution to the wave boundary layer equation (1) depends only slightly on time variation in the eddy viscosity and is more sensitive to a proper treatment of the vertical distribution; the third harmonic of the velocity, present in the velocity field due the time-varying nature of the eddy viscosity, was found to be only a few percent of the first harmonic. In order to avoid the complex mathematics involved when using a time-varying eddy viscosity, the eddy viscosity close to the bed can be simplified by replacing $|u_*|$ by a characteristic constant $u_{*,\text{char}}$.

On the contrary, the third harmonic of the bed shear stress was found to be 20-25% of the first harmonic. The lack of higher harmonics in the predictions of a linear model with time-invariant eddy viscosity may significantly underestimate the asymmetry of the bed shear stress and therewith the asymmetry in sediment concentrations and transport. For that reason, in the determination of the bed shear stress a time-variant eddy viscosity will be used as will be addressed later.

Based on the above considerations, for the determination of analytical solutions to Equation (1), the viscosity close to the bed is often taken to increase linearly away from the

bed. Grant and Madsen (1979) used $\nu_{t,f} = \kappa u_{*,\max} z$ over the entire wave boundary layer thickness where $\kappa = 0.4$ is the von Karman's constant and $u_{*,\max}$ is the maximum bed friction velocity which is related to the maximum bed shear stress $\tau_{b,\max}$ via $u_{*,\max} = \sqrt{\tau_{b,\max}/\rho}$. A two layer model was used by Brevik (1981) who combined the Grant and Madsen model close to the bed with a constant eddy viscosity in the outer layer. The two-layer concept is adopted here since it provides the best compromise between accuracy and simplicity; the constant eddy viscosity in the outer layer is not only more realistic than a linearly increasing eddy viscosity but results in simple analytical solutions as well, whereas close to the bed the linearly increasing eddy viscosity is essential for a good representation of velocity and shear stress. The following two-layer model is used:

$$\begin{aligned} \nu_{t,f} &= \kappa u_{*,\text{char}} z && z_0 < z \le \delta, \\ \nu_{t,f} &= \kappa u_{*,\text{char}} \delta && \delta < z, \end{aligned} \tag{5}$$

in which the transition level δ between the two profiles is modelled as:

$$\delta = m \frac{\kappa u_{*,\text{char}}}{\omega}, \tag{6}$$

where ω is the wave cyclic frequency and $u_{*,\text{char}}$ is a characteristic time-invariant shear velocity representing the time-variant turbulence level in the flow. The choices for the characteristic shear velocity and the coefficient m are discussed later. Note that δ directly determines the magnitude of the eddy viscosity in the relatively large outer layer.

Oscillatory velocity solution

Analytical solutions to (1) using the above specified two-layer eddy viscosity profile (5) are in terms of simple exponential functions of z in the outer layer where a height-invariant viscosity is assumed. In the lower layer however, the linearly varying viscosity results in an analytical solution in terms of Kelvin function of zeroth order (e.g. Grant and Madsen, 1979; Brevik, 1981), which are not only time-consuming from a computational point of view but complicate the depth-integration of the sediment fluxes. For small values of $z\omega/\kappa u_{*,\text{char}}$ and $z_0\omega/\kappa u_{*,\text{char}}$ or equivalently close to the bottom and for large values of a_∞/k_b, asymptotic expressions for the zeroth order Kelvin functions may be used to simplify the velocity profile. These assumptions result in a logarithmic velocity profile and a depth-invariant shear stress and were seen to be valid up to $z = \frac{1}{10}\kappa u_{*,\text{char}}/\omega$. Here we use the equivalent assumption that the shear stress is constant to obtain the velocity profile in the lower layer.

Inserting Equation (2) in (1), using the constant stress assumption in the lower layer and the viscosity profile defined by (5), results in the following set of equations:

$$\begin{aligned} \frac{\partial}{\partial z} \kappa u_{*,\text{char}} z \frac{\partial u}{\partial z} &= 0 && z_0 < z \le \delta, \\ \frac{\partial u - u_\infty}{\partial t} &= \kappa u_{*,\text{char}} \delta \frac{\partial^2 u}{\partial z^2} && \delta < z, \end{aligned} \tag{7}$$

In addition to the two boundary conditions (3), we require the velocity and the velocity gradient to be continuous at the transition level δ between lower and outer layer.

Solving the momentum equations (7) proceeds assuming a harmonie time-dependent wave motion specified by its near-bottom velocity:

$$u_\infty(t) = \sum_{n=1}^{n=N} U_{\infty,n} e^{i\omega_n t} + c.c., \tag{8}$$

where $\omega_n = 2\pi/T_n$ is the angular frequency, T_n the harmonic period, N the number of components under consideration, and $i = \sqrt{-1}$. Note that the coefficients $U_{\infty,n}$ are complex which means that phase differences may exist between the various harmonics in the near-bottom velocity and that *c.c.* denotes the complex conjugates to the terms in the series since the resulting quantities must be real-valued.

The complete solution for the velocity profile in the wave boundary layer as a function of time becomes in the lower layer ($z_0 < z \le \delta$):

$$u(z,t) = \frac{\ln\frac{z}{z_0}}{\ln\frac{\delta}{z_0}} \sum_{n=1}^{n=N} U_n(\delta) e^{i\omega_n t} + c.c. = \ln\frac{z}{z_0} \sum_{n=1}^{n=N} \frac{2U_{\infty,n}}{\left[2\ln\frac{\delta}{z_0} + \frac{\delta_n}{\delta}(1-i)\right]} e^{i\omega_n t} + c.c \tag{9}$$

and in the outer layer ($z < \delta$):

$$u(z,t) = \sum_{n=1}^{n=N} \left[U_{\infty,n} + \left\{U_n(\delta) - U_{\infty,n}\right\} e^{-(1+i)\frac{z-\delta}{\delta_n}} \right] e^{i\omega_n t} + c.c \tag{10}$$

where:

$$\delta_n = \sqrt{\frac{2\kappa u_{*,\mathrm{char}}\delta}{\omega_n}} \tag{11}$$

Comparison of velocity predictions of analytical and numerical model

The velocity predictions were compared with the results of the IDV NEREUS wave boundary layer model (Klopman, see Ribberink and Al-Salem, 1995) in which a mixing length approach (see previous section) is used to derive a time-varying eddy viscosity. For the coefficient m and the characteristic shear velocity $u_{*,\mathrm{char}}$ in Equation (11) we used $m = 1/4$ and $u_{*,\mathrm{char}} = u_{*,\mathrm{mean}}$ based on representation of the mean bed shear stress. For a purely sinusoidal shear velocity, we would have $u_{*,\mathrm{mean}} = 1/\sqrt{2}\, u_{*,\mathrm{max}}$. Generally, the characteristic shear velocity $u_{*,\mathrm{char}}$ is chosen to represent the maximum bed shear stress ($u_{*,\mathrm{char}} = u_{*,\mathrm{max}}$) in order to avoid underestimation of the eddy viscosity during the high-velocity portion of the wave cycle when most of the turbulence is generated (Grant and Madsen, 1979). For the predictions of the maximum velocity profile however, we found that $u_{*,\mathrm{char}} = u_{*,\mathrm{mean}}$ gave the best results in the analytical model. The coefficient m can be expected to be in the range of $1/10$ to $1/4$. The value of $1/8$ corresponds to Kajiura's (1964) transition level to the outer layer, whereas the value of $1/4$ corresponds to the optimal level as found by Brevik (1981) which is half the boundary thickness as defined by Jonsson and Carlsen (1976). The latter value of $m = 1/4$ is adopted here as the standard value for m and has been applied in all computations shown in this paper. Somewhat better velocity predictions can be obtained using a smaller

value for m. Note that the assumption of constant shear stress can formally not be expected to be valid up above $z = \frac{1}{10}\kappa u_{*,\mathrm{char}}/\omega$.

A second order Stokes condition is used in the comparison corresponding to the conditions of LOWT test C1 (see Table 1). We determine $u_{*,\max} = \sqrt{f_w/2}\hat{u}_1$ using Swart's (1974) explicit approximation for the wave friction factor to Jonsson's implicit, semi-empirical formula. The influence of the use of $\hat{u}_1$, the amplitude of the first harmonic, rather than the root-mean-square velocity was negligible and more appropriate in the wave tunnel situation used in the net transport model validation.

Figure 1 shows the velocity at different phases with zero phase corresponding to the maximum 'onshore' velocity as well as the amplitudes of the two harmonic components and the root-mean-square velocity. It can be seen that the predictions of the velocity amplitudes by the analytical model are somewhat smaller than the NEREUS predictions. The velocity predictions with the analytical model are quite reasonable, especially when considering the use of this velocity profile for sediment transport predictions.

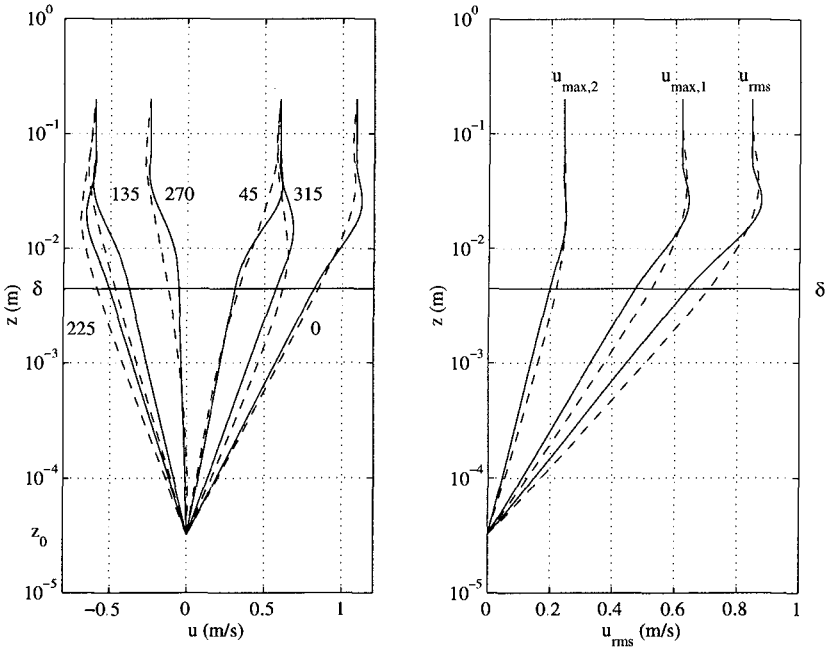

Figure 1 Velocity predictions at different phases and velocity amplitudes (NEREUS dashed lines; analytical model drawn lines). Conditions correspond to test C1 (see Table 1)

Bed shear stress

The bed shear stress resulting from the time-invariant eddy viscosity model is given by:

$$\tau_{b,1} = \lim_{z\to 0}\left(\rho\kappa u_{*,\mathrm{char}} z\frac{\partial u}{\partial z}\right) = \rho\kappa u_{*,\mathrm{char}}\frac{1}{\ln\frac{\delta}{z_0}}\sum_{n=1}^{n=N} U_n(\delta)e^{i\omega_n t} + c.c., \tag{12}$$

from which it can be seen that a linear model with a time-invariant eddy viscosity is obviously not able to predict any higher harmonics in the shear stress field. By choosing $u_{*,\mathrm{char}} = u_{*,\max}$ in a time-invariant model, the maximum bed shear stress can be predicted quite accurately. Trowbridge and Madsen (1984) suggested that a simple way to reproduce in a theoretical model the potentially important third harmonic of the bed shear stress while ignoring the small third harmonic of the velocity would be to compute the velocity field by using a time-invariant eddy viscosity and then compute the bed shear stress by combining the velocity prediction with a time-varying eddy viscosity proportional to a shear velocity based on the instantaneous bed shear stress predicted by the time-invariant model.

This concept is adopted by using the bed shear stress definition (4) which corresponds to a time-variant eddy viscosity model:

$$\tau_{b,2} = \lim_{z\to 0}\left(\rho\kappa\left|u_*(t)\right| z\frac{\partial u}{\partial z}\right) = \lim_{z\to 0}\left(\rho(\kappa z)^2\left|\frac{\partial u}{\partial z}\right|\frac{\partial u}{\partial z}\right) = \rho\frac{\kappa^2}{\left(\ln\frac{\delta}{z_0}\right)^2}\left|u(\delta,t)\right|u(\delta,t), \tag{13}$$

in which the velocity field is obtained using the time-invariant eddy viscosity model (see Equation (9)).

Comparison of shear stress predictions of analytical and numerical model

Figure 2 shows the bed shear stress for both the time-variant and time-invariant eddy viscosity model using $\delta = \frac{1}{4}\kappa u_{*,\mathrm{mean}}/\omega$ as well as $\delta = \frac{1}{8}\kappa u_{*,\max}/\omega$ in comparison with the bed shear stress as computed by NEREUS.

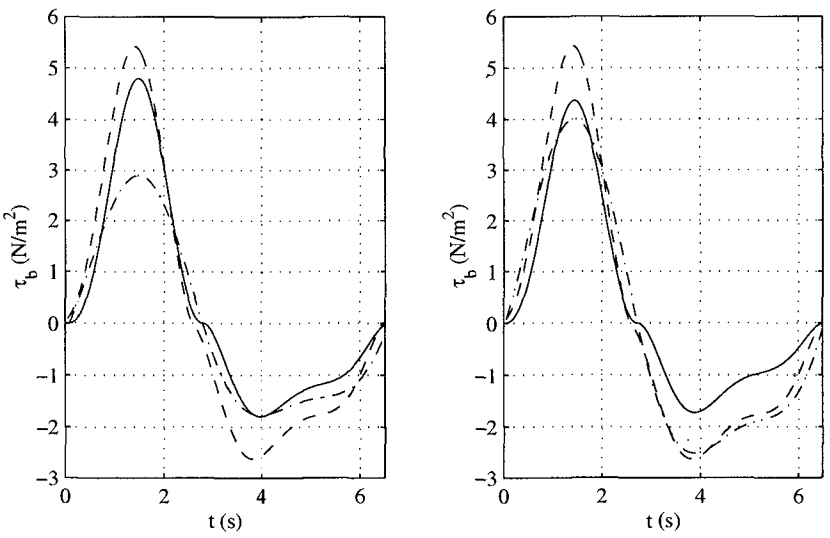

Figure 2 Comparison of bed shear stress for $\delta = \frac{1}{4}\kappa u_{*,\mathrm{mean}}/\omega$ (left) and $\delta = \frac{1}{8}\kappa u_{*,\max}/\omega$ (right) for NEREUS (dashed), time-invariant model (dashed-dot) and time-variant model (drawn)

From Figure 2, it can be seen that for the predictions of the linear model with the time-invariant eddy viscosity, the maximum shear velocity must be used to adequately predict the shear stress amplitude. This could be expected since the shear stress in the linear model is directly proportional to the characteristic shear velocity $u_{*,\mathrm{char}}$, whereas the velocity gradient is less sensitive to the value of $u_{*,\mathrm{char}}$. The predictions using the time-variant model, which are governed by the velocity gradient, are relatively insensitive to $u_{*,\mathrm{char}}$. The most important feature in the predictions of the time-invariant model, is the presence of third and higher harmonics such that the asymmetry of the bed shear stress is in better accordance with NEREUS than the relatively symmetrical bed shear stress as predicted using the time-invariant model. This was found to be extremely important to predict the asymmetry in the sediment concentration at the bed.

Sediment concentration model

Advection-diffusion equation

Conservation of mass is applied to the sediment and the resulting equation is Reynolds averaged. Assuming that the Reynolds averaged vertical water velocity is negligible compared to the fall velocity of the sediment, using the boundary layer approximation and introducing the mass balance for the fluid, yields:

$$\frac{\partial c}{\partial t} + w_s \frac{\partial c}{\partial z} + \frac{\partial \langle c'w' \rangle}{\partial z} = 0, \tag{14}$$

in which c denotes the turbulence averaged concentration, w_s the particle fall velocity (assumed constant) and $-\langle c'w' \rangle$ the turbulence upward sediment flux, where the brackets denote averaging over the turbulence time-scale. In order to model the turbulence sediment flux, we make the assumption of upward transport due to turbulence diffusion as for the fluid, see Equation (2):

$$-\langle c'w' \rangle = \rho \nu_{t,s} \frac{\partial c}{\partial z} \tag{15}$$

in which $\nu_{t,s}$ is the turbulence diffusivity of sediment mass.

The solution to Equation (14) requires two boundary conditions in z. At the water surface the vertical flux is zero which due to the limited extent of the wave boundary layer is normally equivalent to $c \to 0$ for $z \to \infty$. The second boundary condition is related to the bed concentration of the suspended sediment taken at a specified level above the mean bed level. Here we use the reference concentration of Zyserman and Fredsøe (1994) which has the advantage of an upper cut-off for the sediment concentration at large values of the bed shear stress. The sediment concentration is prescribed at a reference level $z_a = 2D_{50}$:

$$c(z_a, t) = c_b(t), \tag{16}$$

Besides, we apply the above boundary condition as a pick-up type boundary condition in which it is the upward diffusive flux from the bed $-\nu_{t,s}\, \partial c / \partial z$ and therefore the concentration gradient rather than the concentration itself which is prescribed:

$$\left(\frac{\partial c}{\partial z}\right)_{z=z_a} = -\frac{w_s}{\left(\nu_{t,s}\right)_{z=z_a}} c_b(t) \tag{17}$$

Diffusivity model

The diffusivity of sediment mass is in principle assumed to follow the same distribution as the diffusivity of fluid momentum, Equations (5). The exact solution in case of a linearly varying diffusivity in the lower layer is in terms of higher order Kelvin functions (Smith, 1977) which are time-consuming to compute and not easily approximated. Therefore, a representative constant diffusivity in the lower layer is used which is determined by requiring the mean concentration at $z = \delta$ to be equal to the mean concentration when using the linearly varying diffusivity. We now have:

$$\begin{aligned} \nu_{t,s} &= \nu_{t,s,1} = \beta \kappa u_{*,\text{char}} \delta \qquad & z_0 < z \le \delta \\ \nu_{t,s} &= \nu_{t,s,2} = \kappa u_{*,\text{char}} \delta \qquad & \delta < z \end{aligned} \tag{18}$$

in which β follows from the above requirement.

In addition, we allow the settling velocity to be different in the two layers. In the lower layer we have $w_s = w_{s,1}$ which is taken as the settling velocity corresponding to the D_{50} of the bed material. In the outer layer, the settling velocity $w_s = w_{s,2}$ can be expected to be smaller, corresponding to $0.7 D_{50} - 0.9 D_{50}$.

Solution

Solving the advection-diffusion equation (14) proceeds assuming a harmonic time-dependent wave motion specified and using complex variables. The general solution in case of a constant diffusivity reads:

$$c(z,t) = \sum_{m=-M}^{m=M} C_m \exp\left(-\alpha_m \frac{w_s}{\nu_{t,s}} z\right) e^{i\omega_m t}, \tag{19}$$

with

$$\alpha_m = \frac{1}{2} + \sqrt{\frac{1}{4} + i\omega_m \frac{\nu_{t,s}}{w_s^2}}, \tag{20}$$

and $M > N$ is the number of harmonic components in the bed concentration. The complex coefficients C_m are determined by the bed boundary condition. With $c_b(z,t) = \sum_{m=-M}^{m=M} C_{b,m} e^{i\omega_m t}$, we find $C_m = C_{b,m}$ and $C_m = C_{b,m}/\alpha_m$ for the concentration-type and gradient-type boundary condition, respectively. At the transition of the lower and outer layer, the concentration is required to be continuous.

Wave-related sediment transport model

Writing the previously found expressions for oscillatory velocity and concentration as $\tilde{u}(z,t) = \sum_{n=1}^{n=N} \zeta_{u,n}(z) e^{i\omega_n t} + cc.$ and $\tilde{c}(z,t) = \sum_{m=1}^{m=M} \zeta_{c,m}(z) e^{i\omega_m t} + cc.$, integration of the

instantaneous flux $\varphi(z,t) = uc$ over time and depth yields for the net wave-related sediment transport:

$$q_{wave} = \frac{1}{t_2 - t_1}\int_{t_1}^{t_2}\int_{z_a}^{\infty}\varphi(z,t)\mathrm{d}z\mathrm{d}t = \int_{z_a}^{\infty}\langle\varphi(z)\rangle\mathrm{d}z = \int_{z_a}^{\infty}\left\{\sum_n \zeta_{u,n}(z)\zeta_{c,-n}(z) + cc.\right\}\mathrm{d}z \tag{22}$$

In the outer layer with a constant diffusivity of fluid momentum and sediment mass, the solutions $\zeta_{u,n}(z)$ and $\zeta_{c,n}(z)$ are in terms of exponential functions such that the integration of the time-averaged flux $\langle\varphi(z)\rangle$ over depth is easily carried out analytically. The linearly increasing diffusivity close to the bed yields a logarithmic profile for $\zeta_{u,n}(z)$ which complicates the analytical integration of $\langle\varphi(z)\rangle$. Therefore a polynomial approximation valid for small values of z is used to approximate the integral.

Herewith we have arrived at a computationally efficient method to account for the wave-related suspended sediment transport taking into account the strong vertical variations in the near-bottom time-varying flow and concentration including the non-instantaneous response of the sediment. With the present time-domain formulation of the bed boundary condition for the sediment, the determination of the net transport rate requires a transformation from frequency to time-domain and vice versa. Compared to using a numerical finite difference scheme however, we have at least a two orders of magnitude reduction in the computational effort.

Comparison with LOWT experiments and results of various models

Description of LOWT experiments

The data used for model validation were obtained by Ribberink and Al-Salem (1994) for dune sand with $D_{50} = 210\mu m$ and by Ribberink and Chen (1993) for finer sand with a $D_{50} = 130\mu m$. The experiments were carried out in the Large Oscillating Water Tunnel. The experiments used here were performed above a plane sand bed for regular asymmetric (2nd order Stokes) waves in the absence of a mean current. The set of experiments covered a range of wave periods, flow velocity and asymmetry (see Table 1). For C1 and D13 (bold in Table 1) detailed time-dependent measurements were performed. For all tests net transport rates were derived using a mass-conservation technique. Time-averaged concentration were measured using a suction system, whereas time-dependent concentrations were measured using a conductivity concentration meter (CCM) in the sheet flow layer and an optical concentration meter (OPCON) in the suspension layer.

The comparison with the experiments was carried out on sediment concentration and time-averaged sediment fluxes for the tests C1 and D13 and on net transport rates for all tests in the respective series. For all tests, the model was run using the standard settings of $\delta = 0.25\kappa u_{*,\mathrm{mean}}/\omega$ and $k_n = 3D_{90}$ and with a fall velocity in the outer layer corresponding to a grain diameter of $0.75D_{50}$ based on grain-size data collected during the experiments. Both the concentration-type and pick-up type concentration boundary conditions were used. Only for D13, a significant difference could be observed in the results of the two boundary conditions.

Series B and C ($D_{50} = 210\mu m$)

In Figure 3, the prediction of the analytical model is compared with the time-varying sediment concentrations at four heights above the original bed level and with the time-

	Tp (s)	u_{rms} (m/s)	$<u^3>$ m^3/s^3		Tp (s)	u_{rms} (m/s)	$<u^3>$ m^3/s^3
B7	6.5	0.5	0.102	D11	6.5	0.56	0.096
B8	6.5	0.7	0.256	D12	6.5	0.91	0.537
B9	6.5	0.92	0.562	D13	6.5	0.73	0.220
B10	9.1	0.54	0.104	D14	6.5	0.45	0.044
B11	9.1	0.70	0.220				
B12	9.1	0.97	0.574				
B13	6.5	0.70	0.114				
B14	9.1	0.71	0.094				
B15	5.0	0.51	0.103				
B16	12.0	0.56	0.101				
C1	6.5	0.59	0.124				

Table 1 Test conditions for B- and C-series (Ribberink and Al-Salem, 1994) and D-series (Ribberink and Chen, 1993).

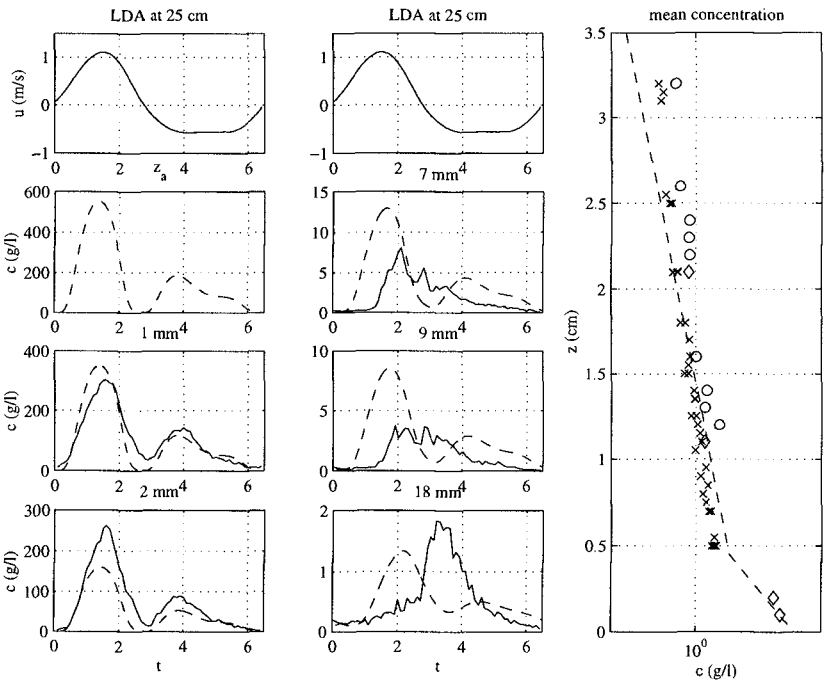

Figure 3 Comparison of measured (drawn) and computed (dashed) sediment concentrations for C1

averaged sediment concentration profile. At the lower levels the predictions are in good agreement regarding amplitude and phase. With distance from the bed especially the phase between the model and data increases. Further, the data show a single-peaked concentration, whereas a second peak is still present in the model predictions. The time-averaged concentration profile is reasonably well predicted. Qualitatively, these features are in agreement with model predictions discussed in a MAST2 G8-M intercomparison study comparing four numerical 1DV models with LOWT data (Davies et al.,1997). In Figure 4 (upper left plot), the predicted time-averaged flux profiles are compared with the data and the

predictions of the Danish STP model based on an eddy viscosity approach (Fredsøe et al., 1985) and a turbulent kinetic energy model (Davies, 1995). The results of the latter two models were taken from the aforementioned paper and were obtained without any fine-tuning of the respective models. Note that for the lower five points measured values for the concentration were combined with estimated values of the velocity, since no velocity measurements were available here. All models and the data show an 'onshore' transport in the near-bed layer and an 'offshore' transport in the outer suspension layer. All models give comparable results and significantly overestimate the height of zero flux and is a direct result of the underestimation of the phase differences between velocity and concentration in the models which are all based on a diffusion approach for the upward transport of sediment.

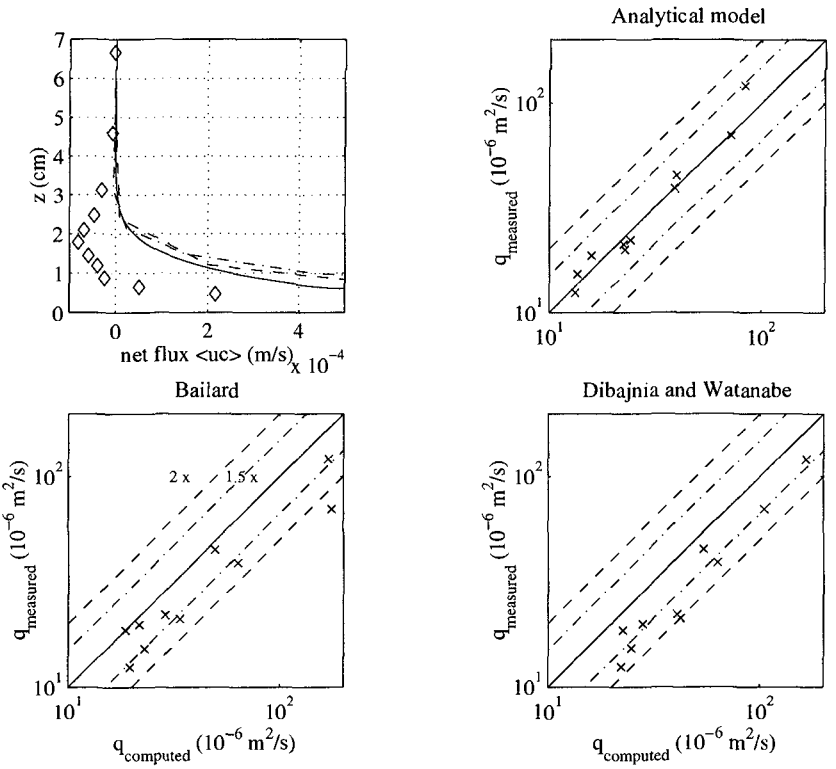

Figure 4 Comparison of measured and computed time-averaged fluxes (upper left plot, STP: dashed, t.k.e.: dashed-dot; analytical: drawn) and comparison of measured and computed net transport rates for various models for the B- and C-series.

The net sediment transport is dominated by the flux in the near-bed layer such that the mismatch between model and data further from the bed can be expected to be relatively unimportant for the net transport predictions. This can be seen in Figure 4, which compares the net transport predictions of the analytical model with the data. Besides, the performance of the Bailard (1981) and Dibajnia and Watanabe (1992) is shown. The latter model results are taken from Janssen et al. (1996). In this figure, perfect agreement corresponds with the 45° line. Also shown are the lines indicating a factor 1.5 and 2 around the line of perfect

agreement. It can be seen that the predictions of the analytical model, the Bailard model and the Dibajnia and Watanabe model are within a factor 2 from the data for 100%, 90 % and 100 % of the tests considered, respectively. Within the band of factor 1.5 we have 100%, 60% and 50% respectively. Also compared to the predictions in Davies et al. (1997), the analytical model gives favourable results.

Series D ($D_{50} = 130\mu m$)

A comparison of the predicted and measured time-varying and time-averaged sediment concentrations, not shown here for brevity, showed many of the features as reported above for test C1. An important difference is the relatively large concentration in the outer layer, such that the predictions in the outer layer are more important to the net sediment transport rate predictions than for the coarser sand.

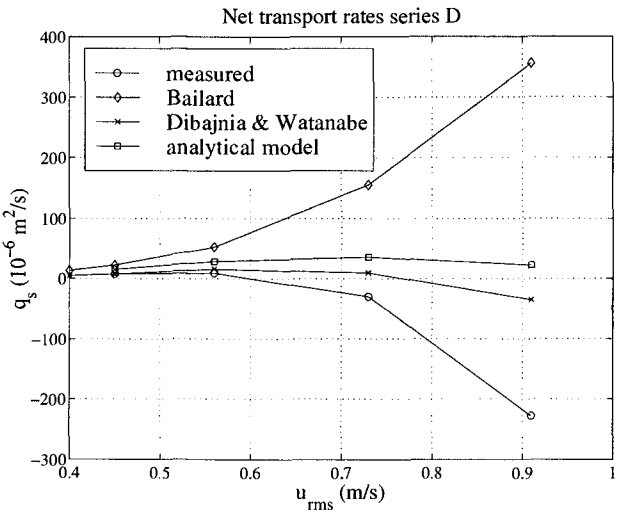

Figure 5 Comparison of measured and computed net transport rates for various models for the D-series

In Figure 5, these net transport rate predictions are compared with the data, together with the predictions of the Bailard and the Dibajnia and Watanabe model (from Janssen et al., 1996). The data show a decreasing and eventually reversing transport rate for increasing root-mean-square velocities. Due to its assumption of quasi-steadiness, the Bailard model cannot follow this trend. Both the analytical model and the Dibajnia and Watanabe model qualitatively follow the observed behaviour, although neither of them predicts the right order of magnitude of the transport rates. The Dibajnia and Watanabe model gives somewhat better results.

Conclusions

The sediment fluxes and net transport rates predicted by the analytical model are comparable to results of numerical 1DV models. However, a considerable reduction of computational effort is obtained. The model gives accurate estimates of the net transport rates for medium sand. For finer sand, although qualitatively correct, the model fails to predict the strong offshore sediment transport rates at higher velocities, mainly due to the diffusion approach.

Acknowledgements

This work is undertaken in the SAFE, FANS and SEDMOC projects, in the framework of the EU-sponsored Marine Science and Technology Programme (MAST-III), under contractno.

MAS3-CT95-0004, MAS3-CT95-0037 and MAS3-CT97-0115, respectively. It is cosponsored by the Dutch Ministry of Transport and Public Works (Rijkswaterstaat) and WL|DELFT HYDRAULICS in the framework of the Netherlands Centre for Coastal Research (NCK).

References

Bailard, J.A, 1981. An energetics total load sediment transport model for a plane sloping beach. *J. of Geophys. Res.*, Vol. 86: C11: 10,938-10,954

Bowen, A.J., 1980. Simple models of nearshore sedimentation; beach profiles and longshore bars. *The Coastline of Canada*, edited by S.B. Cann, pp.1-11, Geological Survey of Canada, Ottawa, 1980

Brevik, I. ,1981. Oscillatory rough turbulent boundary layers. *J. of WatWays, Port, Coastal Ocean Div. Am. Soc. Civ. Engrs*, 107, WW3: 175-188.

Davies, A.G., 1995. Effects of unsteadiness on the suspended sediment flux in co-linear wae-current flow. *Continental Shelf Research*, 15, 8: 949-979.

Davies, A.G., J.S. Ribberink, A. Temperville and J.A. Zyserman, 1997. Comparisons between sediment transport models and observations in wave and current flows above plane beds. *Coastal Engineering*, 31: 163-198.

Dibajnia, M. and A. Watanabe, 1992. Sheet flow under nonlinear waves and currents. *Proc. 23rd Int. Coastal Eng. Conf.*, ASCE, pp. 2015-2028

Fredsøe, J., O.H. Andersen, and S. Silberg, 1985. Distribution of suspended sediment in large waves. *J. of Waterway, Port, Coastal and Ocean Engineering*, 111, 6: 1041-1059.

Grant, W.D. and O.D. Madsen, 1979. Combined wave and current interaction with a rough bottom. *Journal of Geophysical Research*, 84,C4: 1797-1808.

Janssen, C.M. and J.S. Ribberink, 1996. Grain-size influence on sand transport in oscillatory sheet flow. *Proc. 25rd Int. Coastal Eng. Conf.*, ASCE, pp. 4779-4792.

Jonsson, I.G. and N.A. Carlsen, 1976. Experimental and theoretical investigations in an oscillatory sheet flow. *Journal of Hydraulic Research*, 14:45-60.

Kajiura, K., 1964. On the bottom friction in an oscillatory current. *Bull. Earthquake Res. Inst. Uniiv. Tokyo*, 42: 147-174.

Nielsen, P. (1988). Three simple models of wave sediment transport. *Coastal Engineering*, 12: 34-62.

Rakha, K.A., R. Deigaard and I. Brøker, (1997). A phase-resolving cross shore sediment transport model for beach profile evolution. *Coastal Engineering*, 31: 231-261.

Ribberink, J.S. and Z. Chen, 1993. Sediment transport of fine sand under asymmetric oscillatory flow. Data Report H840.20, Part VII, January 1993, WL|DELFT HYDRAULICS, Delft, The Netherlands.

Ribberink, J.S. and A.A. Al-Salem, 1994. Sediment transport in oscillatory boundary layers in cases of rippled beds and sheet flow. *Journal of Geophysical Research*, 99,C6: 12707-12727.

Ribberink, J.S. and A.A. Al-Salem, 1995. Sheet flow and suspension of sand in oscillatory boundary layers. *Coastal Engineering*, 25, 205-225.

Smith, J.D., 1977. Modelling of sediment transport on continental shelves, in *The Sea*, Vol. 6, edited by E.D. Goldberg, I.N. McCave, J.J. O;Brien and J.H. Steele. Pp. 539-577, Interscience, New York, 1977.

Swart, D.H., 1974. Offshore sediment transport and equilibrium beach profiles. WL|DELFT HYDRAULICS, Publ. No. 131.

Trowbridge, J. and O.S. Madsen, 1984. Turbulent wave boundary layers, 1. Model formulation and first-order solution. *Journal of Geophysical Research*, 89,C5: 7989-7997.

Zyserman, J.A. and J. Fredsøe, 1994. Data analysis of bed concentration of suspended sediment. Proc. Am. Soc. Civ. Eng., *Journal of Hydraulic Engineering*, 120(9):1021-1042.